



CHORUS

This is the accepted manuscript made available via CHORUS. The article has been published as:

Near-Unitary Spin Squeezing in ^{171}Yb

Boris Braverman, Akio Kawasaki, Edwin Pedrozo-Peñafiel, Simone Colombo, Chi Shu, Zeyang Li, Enrique Mendez, Megan Yamoah, Leonardo Salvi, Daisuke Akamatsu, Yanhong Xiao, and Vladan Vuletić

Phys. Rev. Lett. **122**, 223203 — Published 5 June 2019

DOI: [10.1103/PhysRevLett.122.223203](https://doi.org/10.1103/PhysRevLett.122.223203)

Near-Unitary Spin Squeezing in ^{171}Yb

Boris Braverman,^{1,* ‡} Akio Kawasaki,^{1,† ‡} Edwin Pedrozo-Peñafiel,^{1,‡} Simone Colombo,¹ Chi Shu,^{1,2} Zeyang Li,¹ Enrique Mendez,¹ Megan Yamoah,¹ Leonardo Salvi,^{1,3} Daisuke Akamatsu,^{1,4} Yanhong Xiao,^{1,5} and Vladan Vuletić^{1, §}

¹*Department of Physics, MIT-Harvard Center for Ultracold Atoms and Research Laboratory of Electronics, Massachusetts Institute of Technology, Cambridge, Massachusetts 02139, USA*

²*Department of Physics, Harvard University, Cambridge, Massachusetts 02138, USA*

³*Dipartimento di Fisica e Astronomia and LENS - Università di Firenze, INFN - Sezione di Firenze, Via Sansone 1, 50019 Sesto Fiorentino, Italy*

⁴*National Metrology Institute of Japan (NMIJ), National Institute of Advanced Industrial Science and Technology (AIST), 1-1-1 Umezono, Tsukuba, Ibaraki 305-8563, Japan*

⁵*Department of Physics, State Key Laboratory of Surface Physics and Key Laboratory of Micro and Nano Photonic Structures (Ministry of Education), Fudan University, Shanghai 200433, China*

(Dated: May 2, 2019)

Spin squeezing can improve atomic precision measurements beyond the standard quantum limit (SQL), and unitary spin squeezing is essential for improving atomic clocks. We report substantial and nearly unitary spin squeezing in ^{171}Yb , an optical lattice clock atom. The collective nuclear spin of $\sim 10^3$ atoms is squeezed by cavity feedback, using light detuned from the system's resonances to attain unitarity. The observed precision gain over the SQL is limited by state readout to 6.5(4) dB, while the generated states offer a gain of 12.9(6) dB, limited by the curvature of the Bloch sphere. Using a squeezed state within 30% of unitarity, we demonstrate an interferometer that improves the averaging time over the SQL by a factor of 3.7(2). In the future, the squeezing can be simply transferred onto the optical clock transition of ^{171}Yb .

PACS numbers: 03.65.Aa, 03.67.Bg, 32.80.Qk

Optical lattice clocks (OLCs) employ ensembles of cold trapped atoms to reach unprecedented fractional accuracy at the level of 10^{-18} [1–5]. Such clocks now operate near the standard quantum limit (SQL) set by quantum projection noise, where the precision of a sensor improves as \sqrt{N} with the number of atoms N . Spin squeezed states (SSSs) [6–22] are many-body entangled states that can overcome the SQL [8, 23]. They have simple Gaussian quasi-probability distributions with reduced (squeezed) and enhanced (antisqueezed) quantum noise, respectively, along two orthogonal directions of the collective atomic spin. While for fixed-bandwidth applications the precision depends on the squeezing alone, André *et al.* [24] have shown that for optimized clocks the antisqueezed direction eventually leaks into the measurement, reducing the gain in precision. In practice, the amount of antisqueezing typically far exceeds the squeezing, and this mechanism can dramatically reduce the precision gain to the point where, e.g., the state with the highest inferred squeezing of 20 dB (and an antisqueezing of 39 dB) [20] would improve the precision of a clock by a mere 2 dB [25]. Thus nearly unitary (area-preserving) squeezing is of high importance for future clock applications. Furthermore, of the most common OLC atoms, spin squeezing in Sr, Ca, Mg or Hg have not been demonstrated so far, and Yb has only been weakly squeezed by ~ 2 dB [10].

In this Letter, we demonstrate for the first time near-unitary optical spin squeezing, as well as the first substantial squeezing in an OLC atom. The observed metro-

logical gain of up to 6.5(4) dB is limited by the state detection, while subtraction of the independently determined measurement noise implies that the generated SSSs offer 12.9(6) dB of metrological gain and 15.9(6) dB of spin noise suppression. Under conditions where the squeezing is unitary within 30%, and nearly optimal for clock applications, we demonstrate an interferometer with a factor of 3.7(2) reduction in averaging time over the SQL. In the future, the demonstrated squeezing between the two nuclear sublevels $|m = \pm \frac{1}{2}\rangle$ of the electronic ground state 1S_0 of ^{171}Yb can be directly used in the OLC by transferring the population of one of the two sublevels into the 3P_0 excited clock state with an optical π pulse [26].

Optical spin squeezing methods rely on the collective interaction of the atomic ensemble with a light field, where for superior performance the atom-light interaction is enhanced by a cavity [15, 19, 20]. One method that does not require detection of the light, which in practice is always imperfect, is cavity feedback squeezing [14, 21, 27]: The spin quantum noise tunes the cavity frequency, such that the amount of light circulating inside the cavity depends on the S_z component of the collective atomic spin. The light then acts back onto another component S_y of the atomic spin through the light shift, creating S_y - S_z quantum correlations and atomic entanglement in the process. In cavity squeezing, any information contained in the light field results in non-unitary evolution of the atomic system [28]. Recently, Zhang *et al.* [29] pointed out that the process can be made more unitary

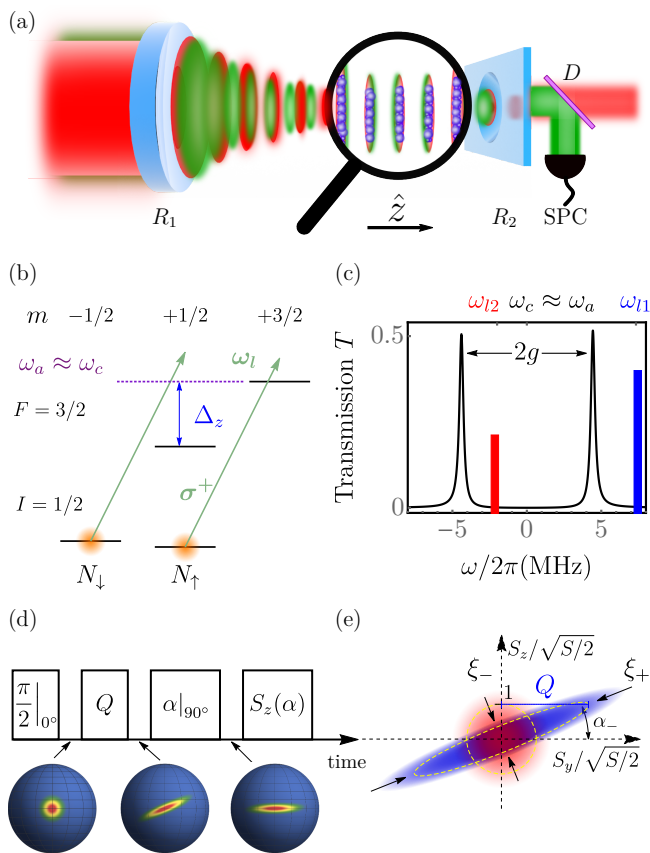


FIG. 1. (a) Experimental setup. A one-dimensional optical lattice at $\lambda_t=759$ nm (red) traps the atoms. Light at $\lambda=556$ nm (green), whose transmission is detected using a dichroic mirror (D) and a single-photon counter (SPC), is used for squeezing and probing. (b) Relevant energy levels of ^{171}Yb with ground state $|^1S_0, I = \frac{1}{2}\rangle$ and excited state $|^3P_1, F = \frac{3}{2}\rangle$. The Zeeman splitting in $|^3P_1, F = \frac{3}{2}\rangle$ is $\Delta_z/(2\pi)=18.5$ MHz for a magnetic field $B_z=13.6$ G along the cavity axis. (c) Cavity transmission spectrum showing vacuum Rabi splitting for $N\eta=1800$, as well as the two squeezing light pulses ω_{l1} and ω_{l2} . (d) Simplified representation of the squeezing and measurement sequence. (e) Quasiprobability distributions for a CSS (red) and SSS (blue).

by detuning the probe light far from cavity resonance. Although this decreases the squeezing strength per photon, it also hides the information about the atomic state in the photon shot noise, thereby enhancing the squeezing. In the present work, we are making use of this idea, but in a resonant regime of vacuum Rabi splitting, rather than dispersive cavity shift [29], resulting in further improved squeezing, and more resilience to technical noise. In addition, we implement spin squeezing on an almost closed optical transition, which removes a squeezing limit due to Raman scattering between the spin states [19, 30], and allows us for the first time to create SSSs that are limited by the curvature of the Bloch sphere for the collective atomic spin (see Fig. 1).

Laser-cooled ^{171}Yb atoms are prepared in a magic-wavelength optical-lattice trap inside an optical cavity. The atom-light interaction is characterized by an effective single-atom cooperativity $\eta=1.8(1)$ and collective cooperativity $N\eta\approx 1800$, where $N\approx 1000$ is the effective atom number (see Ref. [31] and Supplemental Material (SM) [32] for details). The value of the effective cooperativity η is confirmed in an independent measurement.

We perform squeezing between the nuclear sublevels $|\uparrow\rangle \equiv |m_I = \frac{1}{2}\rangle$ and $|\downarrow\rangle \equiv |m_I = -\frac{1}{2}\rangle$ of the electronic 1S_0 ground state of ^{171}Yb . The collective spin state can be represented on a Bloch sphere with radius $S=N/2$ [33]. The cavity frequency is tuned to be nearly resonant with the $|\uparrow\rangle \rightarrow |^3P_1, m_F = \frac{3}{2}\rangle$ atomic transition. N_\uparrow atoms in the state $|\uparrow\rangle$ induce a vacuum Rabi splitting $2g = \sqrt{N_\uparrow\eta\kappa\Gamma}$ of the atom-cavity resonance (Fig. 1(c)), where κ and Γ are the cavity and atomic linewidth, respectively. There is also a small dispersive effect from the N_\downarrow atoms in the state $|\downarrow\rangle$, suppressed by the Zeeman splitting in the excited 3P_1 state, with $\Delta_z \gg \Gamma, \kappa$ (see Fig. 1(b)); this effect is included in our theoretical model (see SM [32] for details).

Since the cavity is primarily coupled to the population N_\uparrow of the state $|\uparrow\rangle$, S_z is determined by detecting N_\uparrow via a measurement of the Rabi splitting $2g$, swapping the populations of $|\uparrow\rangle$ and $|\downarrow\rangle$ with a radiofrequency π pulse, and remeasuring the Rabi splitting to give N_\downarrow . From N_\uparrow and N_\downarrow , we determine $S_z = (N_\uparrow - N_\downarrow)/2$, and $S = (N_\uparrow + N_\downarrow)/2$ using the two-transition atomic model and the separately measured cavity parameters (see SM [32]). The primary quantity of interest, denoted by $\sigma^2 \equiv 2(\Delta S_z)^2/S$, is the spin variance $(\Delta S_z)^2$ normalized to the noise of the coherent spin state (CSS) $(\Delta S_z)_{CSS}^2 = S/2$. The SQL corresponds to $\sigma^2=1$.

The measured spin variance σ^2 is the sum of the variances of the atomic state σ_{st}^2 and the measurement resolution σ_d^2 . To independently quantify the latter, we prepare a CSS on the equator, measure S_z twice, and set $\sigma_d^2 \equiv \text{var}(S_{z1} - S_{z2})/2$. We achieve a detection variance $\sigma_d^2 = -9.4(4)$ dB, i.e. a factor of 9 below the SQL. The measurement quality is limited by a small residual Raman scattering that randomly transfers atoms between the states $|\uparrow\rangle$ and $|\downarrow\rangle$ [19, 20, 27, 30, 34], in combination with the collective cooperativity $N\eta$ and photon detection efficiency $\epsilon = 15\%$ (see SM [32]).

The spin squeezing sequence is shown in Fig. 1(d). First, we create a CSS along the x -axis by optically pumping all atoms into $|\uparrow\rangle$, and then applying a $\pi/2$ -pulse. The squeezing is generated by pulses of light [14, 15], whose frequency ω_l is chosen to balance two competing effects: Increased detuning from the vacuum Rabi peaks makes the squeezing process more unitary with respect to the transmitted light, but also reduces the squeezing per photon and the interferometer contrast (see Fig. 4(b)). Furthermore, fluctuations in the

trapped atom number result in fluctuations of the squeezing strength since the vacuum Rabi splitting depends on N_{\uparrow} , rather than S_z . We cancel this effect by squeezing with bichromatic light inside and outside the Rabi peaks (see Fig. 1(c)), so that the combined squeezing is independent of total atom number. Besides the squeezing, the intracavity light also shifts the phase of the CSS, which we cancel by a spin echo sequence with two bichromatic pulses (see SM [32] for a detailed description).

The generated SSS is reconstructed by rotating it by an angle α about its average spin vector and then detecting the spin projection $S_z(\alpha)$ along the z axis (see Fig. 1(d)). The measurement is repeated more than 100 times for each α . The normalized spin variance $\sigma^2(\alpha) = 2(\Delta S_z(\alpha))^2/S$ along the direction α is displayed in Fig. 2 for several different powers of the squeezing light. As a given SSS is rotated, the projected variance dips below the CSS noise until the rotation angle α reaches α_- , where the short axis of the uncertainty ellipse lies along the z -axis. Beyond α_- , the variance grows until the antisqueezing quadrature is oriented along z for $\alpha = \alpha_- + \pi/2$.

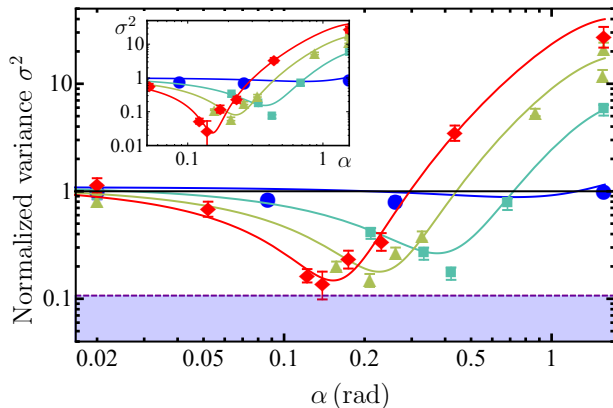


FIG. 2. Measured normalized spin noise $\sigma^2(\alpha)$, as a function of the state rotation angle α , for shearing strengths $Q = 0.3$ (blue circles), $Q = 2.2$ (green squares), $Q = 4.5$ (yellow triangles), and $Q = 6.3$ (red diamonds). For visualization, the data measured at $\alpha=0$ are displayed at $\alpha=0.02$ rad. The solid lines are theoretical fits. States in the violet region below the dashed line at $\sigma^2 = \sigma_d^2 = 0.11$ (detection limit) cannot be directly observed. Inset: σ_{st}^2 of SSS after subtracting measurement noise σ_d^2 for the same parameters.

To compare the data to a theoretical model, we first consider the polar angle of the spin vector, defined as $\tau_\alpha \equiv \sqrt{2S} \arcsin(S_z(\alpha)/S)$. Its variance $(\Delta\tau_\alpha)^2$, normalized to the variance $(\Delta\theta_{CSS})^2 = (2S)^{-1}$ of the CSS, is given by

$$\frac{(\Delta\tau_\alpha)^2}{(\Delta\theta_{CSS})^2} = 1 - Q \sin 2\alpha + (F + Q^2) \sin^2 \alpha. \quad (1)$$

Here, Q is the dimensionless shearing strength (see

Fig. 1(e)), defined as the normalized light-induced phase shift $\pm\phi/\Delta\theta_{CSS}$ experienced by a spin displaced by one standard deviation of the CSS from the equator, $S_z = \pm\sqrt{S/2}$ [14]. The other dimensionless parameter F quantifies the excess broadening (in variance units) compared to a pure SSS or CSS, which have $F = 0$. (For an explicit expression for Q and F see SM [32].)

From Eq. (1) we find the minimum (ξ_-^2) and maximum (ξ_+^2) variances of the normalized spin angle τ_α ,

$$\xi_{\pm}^2 = \frac{1}{2} \left(2 + F + Q^2 \pm \sqrt{4Q^2 + (F + Q^2)^2} \right), \quad (2)$$

obtained at angles $\alpha_- = \arctan[(\sqrt{4Q^2 + (F + Q^2)^2} - (F + Q^2))/(2Q)]$ and $\alpha_+ = \alpha_- + \pi/2$, respectively. The normalized uncertainty area of the SSS ellipse is given by $A = \xi_+ \xi_- = \sqrt{1 + F}$. The relation between $(\Delta\tau_\alpha)^2$ and the normalized spin variance $\sigma^2(\alpha)$ of $S_z(\alpha)$ is given by $\sigma^2(\alpha) = (S/2)[1 - \exp(-2(\Delta\tau_\alpha)^2/S)]$. For the CSS and the SSS quadrature ξ_-^2 , the approximation $\sigma^2(\alpha) \approx (\Delta\tau_\alpha)^2$ holds, while the antisqueezed quadrature ξ_+^2 is reduced by the curvature of the Bloch sphere.

The solid lines in Fig. 2 are obtained by fitting the data to $\sigma^2(\alpha) + \sigma_d^2$ with Q and F as the only fitting parameters, while σ_d^2 is the previously measured detection limit. We find good agreement between the model and the data, allowing us to extract both the shearing strength Q and the excess broadening F . In Fig. 3 we plot Q and F versus the number p_t of transmitted photons during the optical squeezing. For negligible technical noise we expect both Q and F to be proportional to p_t (see SM [32]). The solid lines in Fig. 3 represent the predicted linear behavior of Q and F obtained from an analytical model of the system without any free parameters (see SM [32]); the dotted line includes the effect of finite measurement quality $\sigma_d^2 = -9.4$ dB, that affects the measurement of the squeezed quadrature $\xi_-^2 < 1$, and hence F , but not Q . The model without any free parameters agrees remarkably well with the measured Q and F , indicating the absence of major technical limitations other than the finite state detection quality σ_d^2 .

The attainable metrological gain depends not only on the reduced spin noise ξ_-^2 , but also on the signal $\langle |\vec{S}| \rangle$ [8] which determines the contrast C of an interferometric measurement. The dominant loss of contrast is due to the scattering of photons into free space during squeezing, which projects atoms into $|\uparrow\rangle$ or $|\downarrow\rangle$. The measured Ramsey contrast as a function of Q is shown in Fig. 4, together with the a-priori prediction $C = C_0 \exp(-(Q/\tilde{Q} + Q^2)/N)$ with the initial contrast $C_0 = 0.97$ in the absence of squeezing as the only fitting parameter. Here, $\tilde{Q} = 0.050(3)$ is the independently measured shearing strength per scattered photon. The term Q/\tilde{Q} arises from photon scattering into free space, while the second, smaller term accounts for the SSS wrapping around the Bloch sphere.

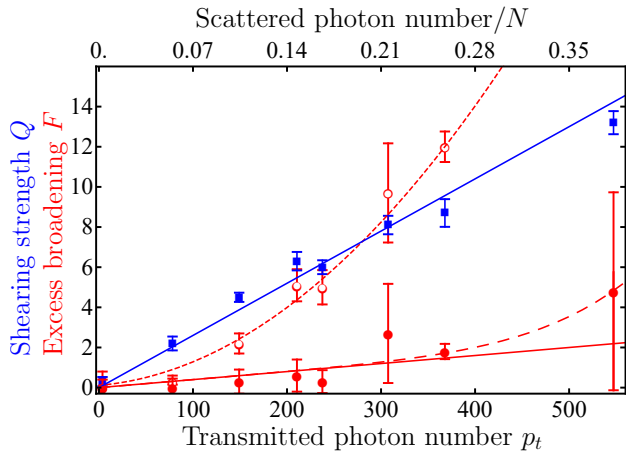


FIG. 3. Shearing strength Q (filled blue squares) and excess broadening factor F (red circles) plotted vs. the number p_t of transmitted photons. The open red circles correspond to the directly measured data with theoretical model without free parameters (dotted red line), the solid circles are after subtraction of measurement noise σ_d^2 with parameter-free model without (solid red line) and with (dashed red line) Bloch-sphere-curvature-induced broadening. The theoretical predictions are given by Eqs. (S7) and (S8) of the SM [32].

The metrological gain of a squeezed state is then given by the Wineland parameter $\xi_W^2 = \xi_-^2 / C^2$ [8]. Fig. 4(a) shows ξ_W^2 , the measured spin noise reduction ξ_-^2 , and the inferred squeezing $\xi_{st}^2 = \xi_-^2 - \sigma_d^2$ of the state after subtraction of the measurement resolution σ_d^2 . For $Q \gtrsim 6$ the measured squeezing ξ_-^2 saturates at σ_d^2 ; $Q=6.3$ also optimizes the Wineland parameter at $\xi_W^2 = -6.5(4)$ dB. The inferred squeezing ξ_{st}^2 is consistent with the prediction from the model with no free parameters (solid red line), which is limited by the Bloch sphere curvature to $\xi_{st}^2 = -15.9(6)$ dB. To our knowledge, this is the first time that the limitation of spin squeezing due to the curvature of the Bloch sphere [6] has been observed. The inferred metrological gain without readout noise is $\xi_W^2 = -12.9(6)$ dB.

Finally, we directly demonstrate an interferometric measurement with a precision beyond the SQL by implementing a Ramsey sequence with a squeezed, nearly uncertainty-limited input state ($Q=3.8$, area $A=\sqrt{1+F}=1.3$). The state is chosen to provide nearly optimum precision gain in the interferometer and in a future OLC [25], see Fig. 4(a). We rotate the squeezed state by $\alpha=\pi/2 - \alpha_-$ to align the minimal uncertainty along the phase axis, allow the state evolve for a Ramsey time $\tau_R=1.5$ ms, and apply a final $\pi/2$ rotation to map the accumulated phase onto S_z . In Fig. 4(c) we compare the phase Allan deviation of the SSS (red squares) with that of the CSS (black circles). The Allan deviation for both CSS and SSS Ramsey sequences is derived from 90 sequential measurements. The precision of the CSS interferometer is accurately described by the SQL (black

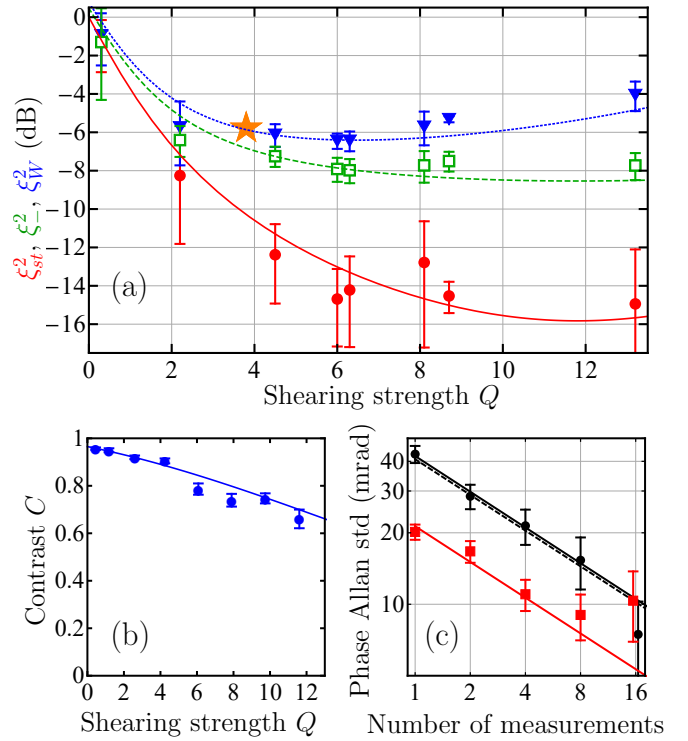


FIG. 4. (a) Wineland metrological gain ξ_W^2 (blue), measured spin noise reduction ξ_-^2 (green), and inferred SSS noise ξ_{st}^2 (red) as a function of shearing strength Q . ξ_-^2 is limited by the measurement resolution and ξ_{st}^2 by the curvature of the Bloch sphere. (b) Ramsey contrast as a function of Q with initial contrast as only fitting parameter (solid line). (c) Allan deviation of a phase measurement for a CSS (black squares) with SQL (dashed line) and for a SSS with $Q=3.8$ ($p_t=130$), $F=0.8$ (red data). The red solid line is fit to the first three data points. The reduction in measurement time over the SQL is a factor of 3.7(2), represented by the orange star in (a).

dashed line). The SSS reaches a given precision 4 times faster than a system at the SQL. The main limitation to longer integration times is magnetic field noise (see SM [32]).

In conclusion, we have demonstrated near-unitary cavity feedback squeezing. Our measurements agree with a model without free parameters that predicts both the area and shape of the squeezed state. The results presented here can be further improved upon in several ways: state detection with a larger applied magnetic field will reduce the Raman scattering and improve the measured spin noise and metrological gain. Alternatively, one can use a squeezing-unsqueezing method [21, 35] that is not limited by the detection quality, and that is also insensitive to the curvature of the Bloch sphere. The intrinsic squeezing of $\xi_{st}^2 = -16$ dB is already more than halfway (on a logarithmic scale) between the SQL and the ultimate Heisenberg limit at $\xi_H^2 = -30$ dB for $N=10^3$ atoms. The squeezing performance depends only on the collec-

tive cooperativity $N\eta$, and by placing the ensemble at a location in the cavity with higher single-atom cooperativity at constant $N\eta$, i.e., for smaller atom number, the demonstrated performance could already be quite close to the Heisenberg limit. Furthermore, the absolute squeezing will improve with increased collective cooperativity in proportion to $N\eta$. We expect that the spin squeezing can be transferred from the nuclear spin directly to the $|^1S_0\rangle \rightarrow |^3P_0\rangle$ clock transition through an optical π pulse, thus enabling optical-clock operation beyond the SQL. Finally, unitary squeezing can also be used to enable quantum information processing with Gaussian states [36, 37].

We would like to thank Monika Schleier-Smith, James Thompson, and Mikhail Lukin for valuable discussions. This work was supported by NSF, DARPA, ONR, and the NSF Center for Ultracold Atoms (CUA). S. C. acknowledges support as a SNSF Early Postdoc.Mobility fellow. B. B. acknowledges the support of the Banting Postdoctoral Fellowship.

* bbraverm@uottawa.ca; Current address: Department of Physics and Max Planck Centre for Extreme and Quantum Photonics, University of Ottawa, 25 Templeton Street, Ottawa, Ontario K1N 6N5, Canada

† akiok@stanford.edu; Current address: W. W. Hansen Experimental Physics Laboratory and Department of Physics, Stanford University, Stanford, California 94305, USA

‡ These authors contributed equally

§ vuletic@mit.edu

- [1] A. D. Ludlow, M. M. Boyd, J. Ye, E. Peik, and P. O. Schmidt, *Rev. Mod. Phys.* **87**, 637 (2015).
- [2] I. Ushijima, M. Takamoto, M. Das, T. Ohkubo, and H. Katori, *Nat. Photonics* **9**, 185 (2015).
- [3] S. L. Campbell, R. B. Hutson, G. E. Marti, A. Goban, N. Darkwah Oppong, R. L. McNally, L. Sonderhouse, J. M. Robinson, W. Zhang, B. J. Bloom, and J. Ye, *Science* **358**, 90 (2017).
- [4] W. F. McGrew, X. Zhang, R. J. Fasano, S. A. Schäffer, K. Beloy, D. Nicolodi, R. C. Brown, N. Hinkley, G. Milani, M. Schioppo, T. H. Yoon, and A. D. Ludlow, *Nature (London)* **564**, 87 (2018).
- [5] G. E. Marti, R. B. Hutson, A. Goban, S. L. Campbell, N. Poli, and J. Ye, *Phys. Rev. Lett.* **120**, 103201 (2018).
- [6] M. Kitagawa and M. Ueda, *Phys. Rev. A* **47**, 5138 (1993).
- [7] D. J. Wineland, J. J. Bollinger, W. M. Itano, F. L. Moore, and D. J. Heinzen, *Phys. Rev. A* **46**, R6797 (1992).
- [8] D. J. Wineland, J. J. Bollinger, W. M. Itano, and D. J. Heinzen, *Phys. Rev. A* **50**, 67 (1994).
- [9] J. Ma, X. Wang, C.-P. Sun, and F. Nori, *Phys. Rep.* **509**, 89 (2011).
- [10] T. Takano, M. Fuyama, R. Namiki, and Y. Takahashi, *Phys. Rev. Lett.* **102**, 033601 (2009).
- [11] J. Appel, P. J. Windpassinger, D. Oblak, U. B. Hoff, N. Kjærgaard, and E. S. Polzik, *Proc. Natl. Acad. Sci. U.S.A.* **106**, 10960 (2009).
- [12] J. Estève, C. Gross, A. Weller, S. Giovanazzi, and M. Oberthaler, *Nature (London)* **455**, 1216 (2008).
- [13] M. F. Riedel, P. Böhi, Y. Li, T. W. Hänsch, A. Sinatra, and P. Treutlein, *Nature (London)* **464**, 1170 (2010).
- [14] I. D. Leroux, M. H. Schleier-Smith, and V. Vuletić, *Phys. Rev. Lett.* **104**, 073602 (2010).
- [15] M. H. Schleier-Smith, I. D. Leroux, and V. Vuletić, *Phys. Rev. Lett.* **104**, 073604 (2010).
- [16] C. D. Hamley, C. Gerving, T. Hoang, E. Bookjans, and M. S. Chapman, *Nat. Phys.* **8**, 305 (2012).
- [17] J. G. Bohnet, B. C. Sawyer, J. W. Britton, M. L. Wall, A. M. Rey, M. Foss-Feig, and J. J. Bollinger, *Science* **352**, 1297 (2016).
- [18] H. Bao, J. Duan, P. Li, X. Lu, W. Qu, M. Wang, I. Novikova, E. Mikhailov, K.-F. Zhao, H. Shen, and Y. Xiao, *arXiv:1811.06945* (2018).
- [19] K. C. Cox, G. P. Greve, J. M. Weiner, and J. K. Thompson, *Phys. Rev. Lett.* **116**, 093602 (2016).
- [20] O. Hosten, N. J. Engelsen, R. Krishnakumar, and M. A. Kasevich, *Nature (London)* **529**, 505 (2016).
- [21] O. Hosten, R. Krishnakumar, N. J. Engelsen, and M. A. Kasevich, *Science* **352**, 1552 (2016).
- [22] R. J. Sewell, M. Koschorreck, M. Napolitano, B. Dubost, N. Behbood, and M. W. Mitchell, *Phys. Rev. Lett.* **109**, 253605 (2012).
- [23] L. Pezzè, A. Smerzi, M. K. Oberthaler, R. Schmied, and P. Treutlein, *Rev. Mod. Phys.* **90**, 035005 (2018).
- [24] A. André, A. S. Sørensen, and M. D. Lukin, *Phys. Rev. Lett.* **92**, 230801 (2004).
- [25] B. Braverman, A. Kawasaki, and V. Vuletić, *New J. Phys.* **20**, 103019 (2018).
- [26] N. D. Lemke, A. D. Ludlow, Z. W. Barber, T. M. Fortier, S. A. Diddams, Y. Jiang, S. R. Jefferts, T. P. Heavner, T. E. Parker, and C. W. Oates, *Phys. Rev. Lett.* **103**, 063001 (2009).
- [27] M. H. Schleier-Smith, I. D. Leroux, and V. Vuletić, *Phys. Rev. A* **81**, 021804(R) (2010).
- [28] I. D. Leroux, M. H. Schleier-Smith, H. Zhang, and V. Vuletić, *Physical Review A* **85**, 013803 (2012).
- [29] Y.-L. Zhang, C.-L. Zou, X.-B. Zou, L. Jiang, and G.-C. Guo, *Phys. Rev. A* **91**, 033625 (2015).
- [30] M. Saffman, D. Oblak, J. Appel, and E. S. Polzik, *Phys. Rev. A* **79**, 023831 (2009).
- [31] A. Kawasaki, B. Braverman, E. Pedrozo-Peñafiel, C. Shu, S. Colombo, Z. Li, O. Özel, W. Chen, L. Salvi, A. Heinz, D. Levonian, D. Akamatsu, Y. Xiao, and V. Vuletić, *Phys. Rev. A* **99**, 013437 (2019).
- [32] See supplemental material at xxx link for additional information, which includes Refs. [38–47].
- [33] J. Hu, W. Chen, Z. Vendeiro, H. Zhang, and V. Vuletić, *Phys. Rev. A* **92**, 063816 (2015).
- [34] Z. Chen, J. G. Bohnet, J. M. Weiner, K. C. Cox, and J. K. Thompson, *Phys. Rev. A* **89**, 043837 (2014).
- [35] E. Davis, G. Bentsen, and M. Schleier-Smith, *Phys. Rev. Lett.* **116**, 053601 (2016).
- [36] C. Weedbrook, S. Pirandola, R. García-Patrón, N. J. Cerf, T. C. Ralph, J. H. Shapiro, and S. Lloyd, *Rev. Mod. Phys.* **84**, 621 (2012).
- [37] T. Opatrný, *Phys. Rev. Lett.* **119**, 010502 (2017).
- [38] A. Kawasaki, B. Braverman, Q. Yu, and V. Vuletić, *J. Phys. B* **48**, 155302 (2015).
- [39] H. Tanji-Suzuki, I. D. Leroux, M. H. Schleier-Smith, M. Cetina, A. T. Grier, J. Simon, and V. Vuletić, in *Advances in Atomic, Molecular, and Optical Physics*,

- Vol. 60, edited by P. B. E. Arimondo and C. Lin (Academic Press, 2011) pp. 201 – 237.
- [40] M. G. Raizen, R. J. Thompson, R. J. Brecha, H. J. Kimble, and H. J. Carmichael, *Phys. Rev. Lett.* **63**, 240 (1989).
- [41] P. Münstermann, T. Fischer, P. Maunz, P. W. H. Pinkse, and G. Rempe, *Phys. Rev. Lett.* **82**, 3791 (1999).
- [42] E. J. Davis, G. Bentsen, L. Homeier, T. Li, and M. H. Schleier-Smith, *Phys. Rev. Lett.* **122**, 010405 (2019).
- [43] B. Braverman, *Cavity Quantum Electrodynamics with Ensembles of Ytterbium-171*, Ph.D. thesis, Massachusetts Institute of Technology (2018).
- [44] H. K. Cummins, G. Llewellyn, and J. A. Jones, *Phys. Rev. A* **67**, 042308 (2003).
- [45] M. Bando, T. Ichikawa, Y. Kondo, and M. Nakahara, *J. Phys. Soc. Jpn.* **82**, 014004 (2013).
- [46] B. Braverman, A. Kawasaki, E. Pedrozo-Peñafiel, C. Shu, S. Colombo, Z. Li, and V. Vuletić, (2019), manuscript in preparation.
- [47] A. Kawasaki, *Towards Spin Squeezed ^{171}Yb Atomic Clock beyond the Standard Quantum Limit*, Ph.D. thesis, Massachusetts Institute of Technology (2017).